

The irradiated ISM of ULIRGs

M. Spaans¹, R. Meijerink², F.P. Israel³, A.F. Loenen^{1,4}, W.A. Baan⁴

¹Kapteyn Astronomical Institute, P.O. Box 800, 9700 AV Groningen, The Netherlands
email: spaans@astro.rug.nl

²Astronomy Department, University of California, Berkeley, CA 94720, United States

³Leiden Observatory, P.O. Box 9513, 2300 RA Leiden, The Netherlands

⁴ASTRON, P.O. Box 2, 7990 AA Dwingeloo, The Netherlands

Abstract. The nuclei of ULIRGs harbor massive young stars, an accreting central black hole, or both. Results are presented for molecular gas that is exposed to X-rays (1-100 keV, XDRs) and far-ultraviolet radiation (6-13.6 eV, PDRs). Attention is paid to species like HCO⁺, HCN, HNC, OH, H₂O and CO. Line ratios of HCN/HCO⁺ and HNC/HCN discriminate between PDRs and XDRs. Very high J (> 10) CO lines, observable with HIFI/Herschel, discriminate very well between XDRs and PDRs. In XDRs, it is easy to produce large abundances of warm ($T > 100$ K) H₂O and OH. In PDRs, only OH is produced similarly well.

Keywords. ISM: molecules – galaxies: evolution

1. Introduction

The power that emanates from (ultra-)luminous infrared galaxies is believed to stem from active star formation and/or an accretion disk around a central super-massive black hole (e.g. Sanders & Mirabel 1996). The unambiguous identification of the central energy source, or the relative contributions from stars and an active galactic nucleus (AGN), remains a major challenge in the study of active galaxy centers (Aalto et al. 2007). Molecular lines are ideal in this to penetrate deep into the large column density regions of active galaxies (Israel 2005; Baan & Klöckner 2005). The interested reader is referred to Meijerink & Spaans (2005) and Meijerink, Spaans & Israel (2006, 2007) for details on Photon-Dominated Region (PDR) and X-ray Dominated Region (XDR) physics. PDRs refer to the presence of a starburst that produces photons with energies of 6-13.6 eV, while XDRs indicate an accreting black hole with photon energies of 1-100 keV (Maloney et al. 1996; Lepp & Dalgarno 1996). The most important thing to realize is that a 1 keV photon penetrates a hydrogen column of about 10^{22} cm⁻², while a UV photon (10 eV) is absorbed by dust after about 1 mag of visual extinction. This is a consequence of the fact that X-ray absorption cross sections scale roughly like energy⁻³, allowing deep penetration of X-rays into interstellar clouds.

2. Results

All presented models are plane-parallel slabs and are parameterized by a constant density and an impinging UV (in multiples of $G_0 = 1.6 \times 10^{-3}$ erg s⁻¹ cm⁻²) or X-ray (energy^{-0.9}) radiation field F_X in erg s⁻¹ cm⁻². Note that a flux of $F_X = 100$ erg s⁻¹ cm⁻² corresponds to a 10^{44} erg s⁻¹ Seyfert nucleus at 100 pc from an interstellar cloud.

It is clear from figures 1, 2, 3 and 4 that OH is easily formed in PDRs and XDRs, while warm water is present mostly in XDRs. In PDRs, OH is the dissociation product of water, while it is formed indirectly through charge transfer of H⁺ and O, rapid reactions with H₂

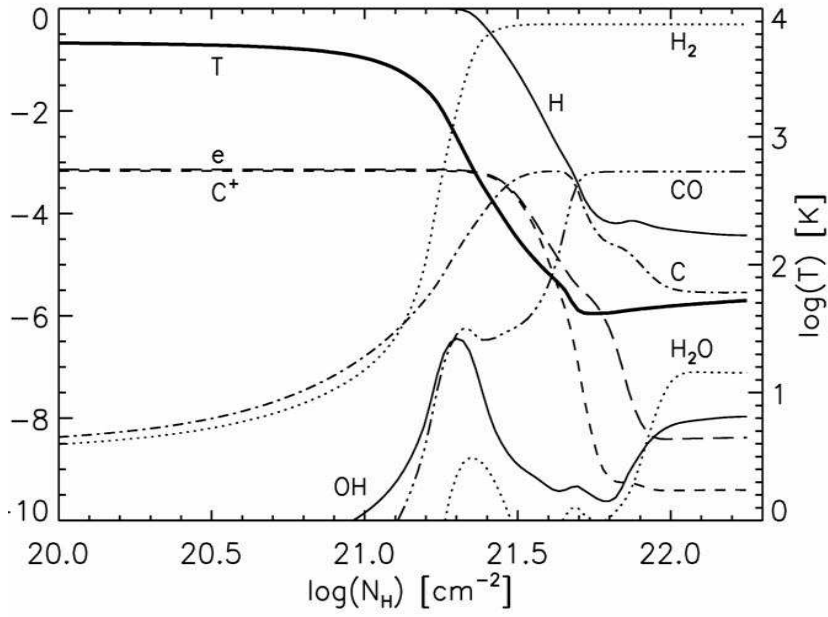


Figure 1. Depth dependence of a few important chemical species in the PDR, $n = 10^5 \text{ cm}^{-3}$ and $10^{3.5} G_0$. Note the clear stratification.

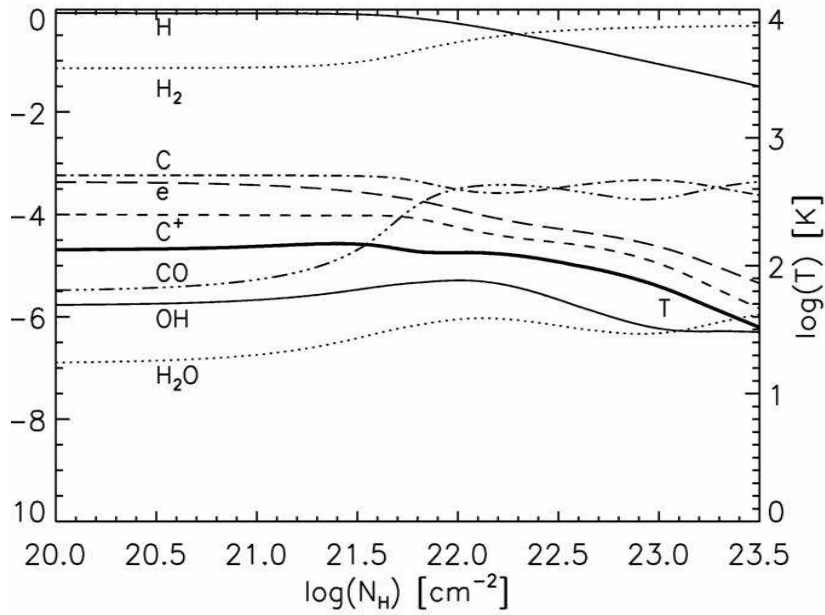


Figure 2. Depth dependence of a few important chemical species in the XDR, $n = 10^5 \text{ cm}^{-3}$ and $F_X = 5 \text{ erg s}^{-1} \text{ cm}^{-2}$. Note the different column density scale and warm water.

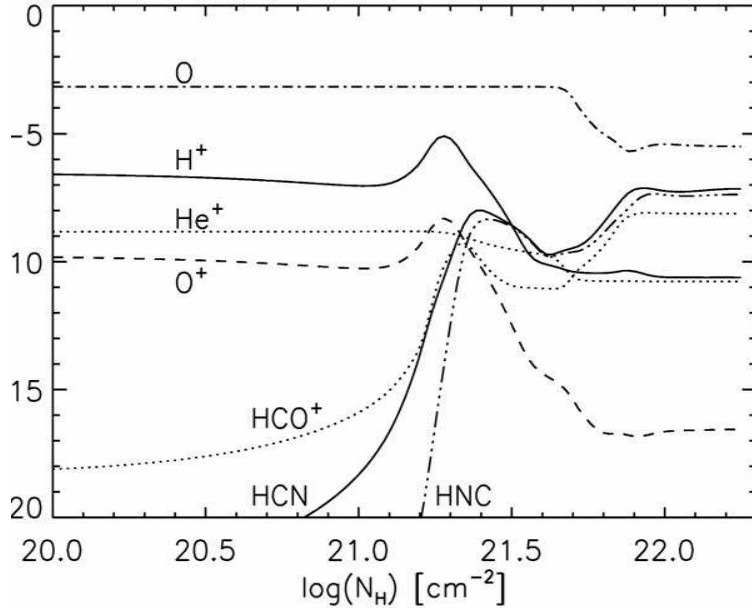


Figure 3. Depth dependence of a few important species in the PDR, same as figure 1.

to OH^+ and H_2O^+ , followed by dissociative recombination or directly through $\text{O} + \text{H}_2 \rightarrow \text{OH} + \text{H}$. The latter reaction is driven efficiently above 200 K. Additional reactions of H_2O^+ with molecular hydrogen lead to H_3O^+ which dissociatively recombines to, among others, water or OH. Note that an elevated cosmic ray ionization rate also leads to larger abundances of H_3O^+ , but not to the same degree as in XDRs (Meijerink et al. 2006). In both PDRs and XDRs, vibrationally excited H_2 is also present through, respectively, UV pumping and thermal collisions with electrons. This significantly lowers the effective energy barrier of the $\text{O} + \text{H}_2$ reaction. In XDRs, an internal UV radiation field is created by collisional excitation of H and H_2 that leads to Lyman α and Lyman-Werner photons through radiative decay. However, this UV field is not strong enough to dissociate water as efficiently as in PDRs. At the high temperatures reached in XDRs, because photoionization heating is more efficient than photo-electric heating by dust grains, the endothermic reaction $\text{OH} + \text{H}_2$ also leads to water. Of course, shocks are similarly capable of producing OH and H_2O .

Typically, the HCO^+ lines are stronger in XDRs than in PDRs by a factor of at least three. This is a direct consequence of the higher ionization degree in XDRs (Meijerink & Spaans 2005), leading to an enhanced HCO^+ formation rate. Depending on the incident radiation field, HCN or HCO^+ is more abundant at the PDR edge of the cloud. At sufficiently large column and densities, the $\text{HCN}(1-0)/\text{HCO}^+(1-0)$ ratio becomes larger than 1. In the XDR models, HCO^+ is chemically less abundant than HCN for very large H_X/n (Meijerink & Spaans 2005). However, for larger columns HCO^+ always becomes more abundant than HCN (Fig. 10 in Meijerink & Spaans 2005). These effects are summarized in figure 2, 4 and 5, see also Loenen et al. (this volume).

The critical densities of HCN and HNC are almost identical, so the only differences in ratios can be due to differences in the abundances. It turns out that the HNC/HCN column density ratio is quite close to that of $\text{HNC}(1-0)/\text{HCN}(1-0)$ line intensity ratio. In

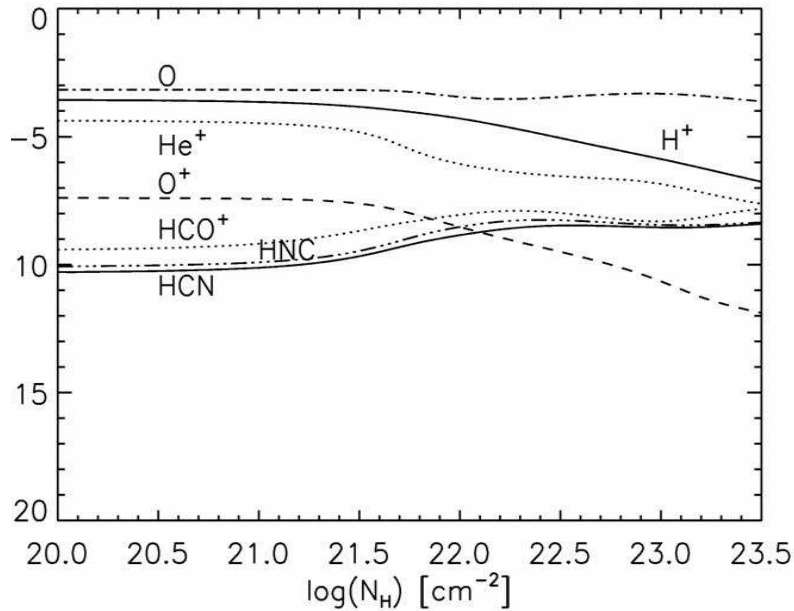


Figure 4. Depth dependence of a few important species in the XDR, same as figure 2. Note the enhancement of HNC with respect to HCN (factor 2).

PDRs, HCN is more abundant in the radical region, but deeper into the cloud the ratio becomes about one. In XDRs, HCN is more abundant in the highly ionized part of the cloud. However, HNC is equally or even more abundant than HCN deep into the cloud. All this can be seen in figures 2 and 4.

In XDRs at high densities CO is present all throughout the cloud, even when F_X/n is large. This is a direct consequence of the fact that X-rays do not lead to strong dissociation of CO and thus C^+ , C and CO typically co-exist in an XDR at elevated (> 100 K) temperatures. Such warm CO gas produces emission originating from high rotational transitions. Contrary to XDRs, most CO in PDRs is produced after the H/H_2 transition and has on average much lower temperatures ($T \sim 20 - 50$ K). Future missions such as Herschel/HIFI will be able to distinguish between PDRs and XDRs by observing high rotational transitions such as CO(16-15), see figure 6.

3. Future work

In the future, observatories like Herschel and ALMA will revolutionize our understanding of the nuclear activity in (maser) galaxies by resolving the central regions of these systems spatially. In this light, it is important to stress that starburst activity typically occupies a larger fraction of an active galaxy than accretion onto a central black hole. Consequently, single dish observations are likely to be dominated by a PDR signal even when an XDR is present. This is particularly true for the very high J CO lines and emphasizes the need for high spatial resolution. ALMA can detect and resolve very high J CO emission from ULIRGs at redshifts beyond eight. Additional molecules that allow one to probe an accreting black buried inside ULIRGs, i.e. that are direct tracers of X-ray irradiation, are CO^+ , CH^+ and H_3^+ .

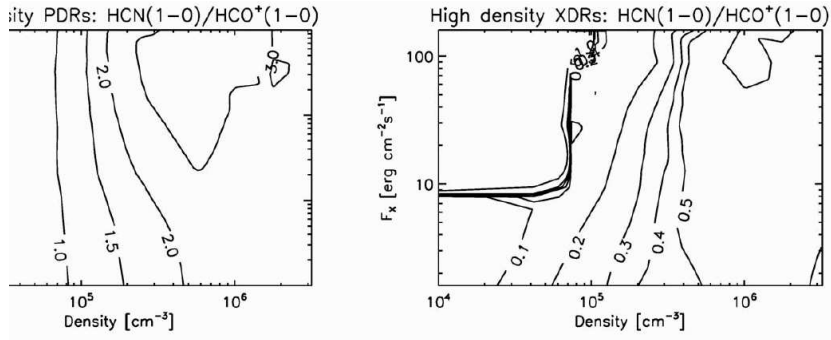


Figure 5. The HCN(1-0)/HCO⁺(1-0) line intensity ratio for a grid of PDR (left) and XDR (right) models.

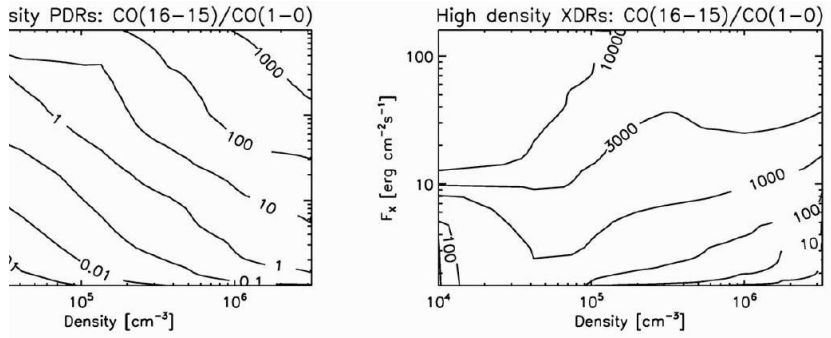


Figure 6. The CO(16-15)/CO(1-0) line intensity ratio for a grid of PDR (left) and XDR (right) models.

Acknowledgements

We are grateful to Dieter Poelman and Juan Pablo Pérez-Beaupuits for discussions.

References

- Aalto, S., Spaans, M., Wiedner, M.C., & Hüttemeister, S., 2007, *A&A* 464, 193
 Baan, W.A. & Klöckner, H.-R., 2005, *Ap&SS*, 295, 263
 Israel, F.P., 2005, *Ap&SS*, 295, 171
 Lepp, S. & Dalgarno, A., 1996, *A&A*, 306, L21
 Maloney, P.R., Hollenbach, D.J., & Tielens, A.G.G.M., 1996, *ApJ*, 466, 561
 Meijerink, R. & Spaans, M., 2005, *A&A*, 436, 397
 Meijerink, R., Spaans, M., & Israel, F.P., 2006, *ApJL*, 650, L103
 Meijerink, R., Spaans, M., Israel, F.P., 2007, *A&A*, 461, 793
 Sanders, D.B. & Mirabel, I.F., 1996, *ARA&A*, 34, 749